AAPS PharmSciTech, Vol. 13, No. 4, December 2012 (© 2012)
DOI: 10.1208/s12249-012-9853-9

Research Article

Enhanced Antiproliferative Activity of the New Anticancer Candidate LPSF/AC04 in Cyclodextrin Inclusion Complexes Encapsulated into Liposomes

Elisângela A. M. Mendonça,[1,2] Mariane C. B. Lira,[2,3] Marcelo M. Rabello,[4] Isabella M. F. Cavalcanti,[2] Suely L. Galdino,[5] Ivan R. Pitta,[5] Maria do Carmo A. Lima,[5] Maira G. R. Pitta,[6] Marcelo Z. Hernandes,[4] and Nereide S. Santos-Magalhães[3,7]

Received 12 April 2012; accepted 10 September 2012; published online 2 October 2012

Abstract. LPSF/AC04 (5Z)-[5-acridin-9-ylmethylene-3-(4-methyl-benzyl)-thiazolidine-2,4-dione] is an acridine-based derivative, part of a series of new anticancer agents synthesized for the purpose of developing more effective and less toxic anticancer drugs. However, the use of LPSF/AC04 is limited due to its low solubility in aqueous solutions. To overcome this problem, we investigated the interaction of LPSF/AC04 with hydroxypropyl-β-cyclodextrin (HP-β-CyD) and hydroxypropyl-γ-cyclodextrin (HP-γ-CyD) in inclusion complexes and determine which of the complexes formed presents the most significant interactions. In this paper, we report the physical characterization of the LPSF/AC04–HP-CyD inclusion complexes by thermogravimetric analysis, differential scanning calorimetry, infrared spectroscopy absorption, Raman spectroscopy, ^{1}HNMR, scanning electron microscopy, and by molecular modeling approaches. In addition, we verified that HP-β-CyD complexation enhances the aqueous solubility of LPSF/AC04, and a significant increase in the antiproliferative activity of LPSF/AC04 against cell lines can be achieved by the encapsulation into liposomes. These findings showed that the nanoencapsulation of LPSF/AC04 and LPSF/AC04–HP-CyD inclusion complexes in liposomes leads to improved drug penetration into the cells and, as a result, an enhancement of cytotoxic activity. Further *in vivo* studies comparing free and encapsulated LPSF/AC04 will be undertaken to support this investigation.

KEY WORDS: acridine; cyclodextrins; cytotoxicity; liposomes; modeling.

INTRODUCTION

Acridine derivatives have a long and successful history in the treatment of human diseases, particularly for parasite infections and cancer (1–3). A variety of acridine derivatives has been synthesized and, in some cases, promising results have been obtained, prompting the development of new acridine-based drugs (3). The major example of these molecules is *m*-amsacrine, a well-known anticancer agent used to treat some types of cancers, including acute adult leukemia (1,4). Their strong activity was due to the ability of acridine nucleus to intercalate into DNA base pairs. This intercalative property has been attributed to the planar aromatic system of the acridine moiety (5).

LPSF/AC04 (5Z)-[5-acridin—9-ylmethylene-3-(4-methyl-benzyl)-thiazolidine-2,4-dione] (Fig. 1) is a synthetized acridinylidene thiazolidinedione, a monoacridinine structural analogue of *m*-amsacrine (6). LPSF/AC04 revealed antitumor activity with tumor inhibition of more than 85% in a murine sarcoma 180 model after 8 days of treatment with 100 mg/kg i.p./day (7). In addition, a recent study presented a preliminary pharmacokinetics of LPSF/AC04 with a half-life of 66 h, which accumulated in different tissues (8). However, heterocyclic acridine derivatives such as LPSF/AC04 are characterized by low solubility in aqueous solutions, as a result of which clinical trials and its therapeutic use have remained limited.

Cyclodextrins (CyDs) have a relatively nonpolar cylindrical cavity that can bind, and thereby solubilize, a wide range of hydrophobic molecules (9,10). A greater number of reports mentioned the use of cyclodextrins in the formation of inclusion complexes with hydrophobic drugs, including acridine derivatives, for enhancement of their solubility (9–14).

The encapsulation of hydrophobic drugs in nanocarriers, such as liposomes, is also of great importance (15). Moreover, the entrapment of inclusion complexes into drug delivery systems, such as liposomes, can modulate *in vivo* dissociation of the drug/CyD complex, thereby contributing to improvements in the pharmacokinetic profile, chemical stability, and

[1] Laboratório de Síntese e Vetorização de Moléculas, Universidade Estadual da Paraíba (UEPB), João Pessoa, PB, Brazil.
[2] Laboratório de Imunopatologia Keizo-Asami (LIKA), Universidade Federal de Pernambuco (UFPE), Av. Prof. Moraes Rego, 1235, Cidade Universitária, 50670-901 Recife, PE, Brazil.
[3] Centro Acadêmico de Vitoria (CAV), Recife, PE, Brazil.
[4] Laboratório de Química Teórica Medicinal-UFPE, Recife, PE, Brazil.
[5] Laboratório de Planejamento e Síntese de Fármacos-UFPE, Recife, PE, Brazil.
[6] Laboratório de Imunomodulação e Novas Abordagens Terapêuticas-UFPE, Recife, PE, Brazil.
[7] To whom correspondence should be addressed. (e-mail: nereide.magalhaes@gmail.com)

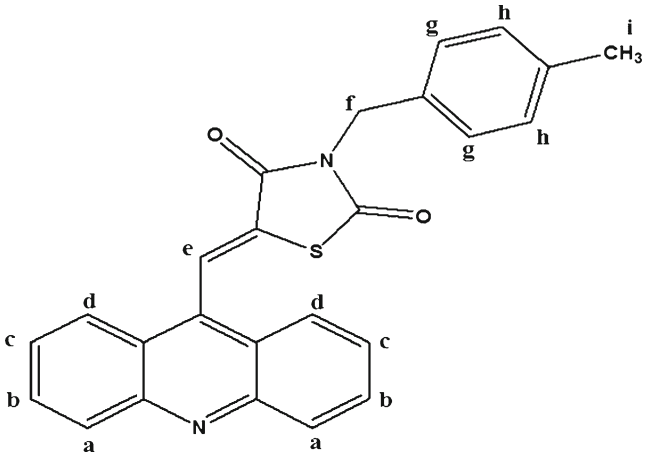

Fig. 1. Chemical structure of LPSF/AC04

therapeutic efficacy of the drugs (16–20). The main purpose of inclusion complex-loaded liposomes is to combine the advantages of cyclodextrins as increasing agents of drug solubility with those of liposomes as drug targeting agents.

The goals of the present study were therefore to assess and characterize using molecular modeling LPSF/AC04–HP-CyD inclusion complexes and to prepare liposomes entrapping LPSF/AC04 or encapsulating LPSF/AC04–HP-CyD inclusion complexes. In addition, the antiproliferative activity of LPSF/AC04 and LPSF/AC04–HP-CyD encapsulated into liposomes in T47D cell line was also evaluated.

EXPERIMENTAL

Materials

LPSF/AC04 obtained by the synthetic route (6) was kindly provided by the Laboratory of Medicinal Chemistry of the Federal University of Pernambuco, Brazil, CAS: 440367-56-6. Cholesterol (CHOL), trehalose, stearylamine (SA), 2-hydroxypropyl-β-cyclodextrin (HP-β-CyD), and 2-hydroxypropyl-γ-cyclodextrin (HP-γ-CyD) were purchased from Sigma-Aldrich (St. Louis, USA). Soybean phosphatidylcholine (SPC, S100®) was obtained from Lipoid GmbH (Ludwigshafen, Germany). Solvents and other chemicals were supplied by Merck (Darmstadt, Germany).

Methodology

Phase Solubility Study of LPSF/AC04 in Cyclodextrin Solutions

A phase solubility assay of LPSF/AC04 in HP-β-CyD and HP-γ-CyD was performed in water at 25°C (21). An excess amount of LPSF/AC04 (3 mg) was added to 1.5 ml of an aqueous CyD solution at concentrations ranging from 0 to the maximal solubility of CyD. The mixtures were shaken vigorously at 25±1°C until equilibrium was attained (about 72 h). Samples were then centrifuged at 8,792×*g* for 10 min and the supernatant filtered (Millex® filter, Millipore, USA). An aliquot (1,000 μl) of the filtrate was removed and analyzed for LPSF/AC04 content using UV spectrophotometry (Ultrospec® 300, Amersham Pharmacia) at 250 nm, with the molar absorption coefficient (ε) of $7.55\times10^4 L mol^{-1} cm^{-1}$. Solubility data were fitted using linear regression. Assuming the formation of a complex with a 1:1 stoichiometric ratio, the apparent stability constant ($K_{1:1}$) of LPSF/AC04 was calculated from the linear relationship between the molar concentration of LPSF/AC04 in the solution medium *versus* the CyD molar concentration according to Eq. 1 (21), where S_0 is the solubility of the LPSF/AC04 in the absence of CyD.

$$K_{1:1} = \frac{slope}{[S_0 \times (1 - slope)]} \quad (1)$$

The complexation efficiency (CE) of LPSF/AC04 was determined from data of the phase solubility curve according to Eq. 2 (9).

$$CE = \frac{slope}{(1 - slope)} \quad (2)$$

Preparation of LPSF/AC04–CyD Inclusion Complexes

LPSF/AC04–CyD inclusion complexes were prepared using the *freeze-drying* technique. Stoichiometric amounts of LPSF/AC04 were dissolved in CyD solutions at 1:1 and 1:2 molar ratios. The mixture was then stirred for 72 h at 25°C and frozen at −80°C. Finally, samples were lyophilized at 4×10^{-6} Barr for 48 h.

Characterization of LPSF/AC04–CyD Inclusion Complexes

Vibrational and Raman Spectroscopic Analyses

Infrared spectra were recorded on a Bruker Vertex 70 FT-IR spectrometer with a spectral resolution of 4 cm^{-1}. KBr pellets of solid samples were prepared from mixtures of 200 mg KBr and 1 mg of sample. FT-Raman spectra were recorded from the samples on a Bruker Ram II spectrometer equipped with a Nd:YAG laser (1,064 nm excitation line) and a liquid-nitrogen cooled Ge detector. FT-Raman spectra were acquired by accumulating 1,024 scans at a spectral resolution of 4 cm^{-1}.

^{1}H-NMR Analysis

Proton NMR (^{1}H-NMR) spectra of LPSF/AC04 and LPSF/AC04–CyDs inclusion complexes were obtained on a Varian Unity Plus 300 MHz NMR spectrometer. The probe temperature was set at 25°C, and the results were processed using the MestReC® software. Experiments were carried out using the following pulse sequences: for the LPSF/AC04 and LPSF/AC04/HP-β-CyD inclusion complexes at the 1:1 and 1:2 molar ratios, a preset (pulse sequence with pre-saturation of water signal in δ 4.72 ppm) with a 90° pulse width and acquisition time of 3.641 s, and for HP-β-CyD, a pulse sequence s2pul with a 45° pulse width and acquisition time of 3.641 s. All samples were solubilized in D_2O. Chemical shifts were reported in parts per million.

Thermal Analysis

Simultaneous thermogravimetric (TGA) and differential thermal analysis (DTA) measurements were performed in a Netzsch STA 409 CD apparatus, coupled to a Bruker Tensor 27 Fourier transform infrared spectrometer. The measurements were performed from 25°C to 500°C at 10°Cmin^{-1}, under nitrogen flow using an open aluminum pan, in which approximately 3 mg of the sample was placed.

Scanning Electron Microscopy Analysis

Scanning electron microscopy (SEM) was performed using Quanta 200F microscopy (FEI Company, Hillsboro, Oregon, USA). Samples of LPSF/AC04, HP-β-CyD and LPSF/AC04–HP-β-CyD inclusion complex were placed in a carbon double-sided tape and fixed on an aluminum stub.

Molecular Modeling of the Inclusion Complexes

In order to elucidate the intermolecular interactions and calculate the interaction energies between LPSF/AC04 and HP-β-CyDs inclusion complexes, molecular modeling techniques were used. There are several reports in the literature using molecular modeling of drugs in HP-β-CyD inclusion complexes (22–25). Our group has already used the latter's methodological approach, for β-lapachone–HP-β-CyD inclusion complexes considering the degree of substitution of hydroxypropyl (HP) groups in the glucose units of β-CyD (20). The total geometry optimizations of the isolated molecules (LPSF/AC04 and HP-β-CyD) and inclusion complexes with one (LPSF/AC04:1×HP-β-CyD) and two (LPSF/AC04:2×HP-β-CyD) HP-β-CyD molecules were computed using the semi-empirical RM1 quantum chemical method, which is part of the Spartan'08 software package (26).

The intermolecular interaction energies (ΔE) for the host–guest inclusion complexes with one ($\Delta E_{\text{bimolecular}}$) or two ($\Delta E_{\text{trimolecular}}$) HP-β-CyD hosts, in addition to one guest (LPSF/AC04) molecule, were calculated by the supermolecule approach, in which the energies of the monomers ($E_{\text{LPSF/AC04}}$ and $E_{\text{HP-β-CyD}}$) were subtracted from the energy of the complexes ($E_{\text{LPSF/AC04:1×HP-β-CyD}}$ or $E_{\text{LPSF/AC04:2×HP-β-CyD}}$), i.e.,

$$\Delta E_{bimolecular} = E_{LPSF/AC04:1\times HP-\beta-CyD} - E_{LPSF/AC04} - E_{HP-\beta-CyD} \quad (3)$$

$$\Delta E_{trimolecular} = E_{LPSF/AC04:2\times HP-\beta-CyD} - E_{LPSF/AC04} - 2 \times E_{HP-\beta-CyD} \quad (4)$$

Preparation of LPSF/AC04-Loaded Liposomes

LPSF/AC04-loaded liposomes were prepared using the thin lipid film method (19). Briefly, lipids (SPC, CHOL, and SA, 7:2:1 molar ratio) at a concentration of 42 mM and LPSF/AC04 (0.4–0.8 mg/ml) were dissolved in a mixture of $CHCl_3$/MeOH (3:1 *v*/*v*) under magnetic stirring. The solvents were removed in a vacuum for 60 min (37±1°C, 80 rpm), resulting in a thin lipid film. This film was then hydrated with 10 ml of pH 7.4 phosphate buffer solution, producing multilamellar liposomes. The liposomal suspension was kept under magnetic stirring for 5 min and was then sonicated (Vibra Cell, Branson, USA) at 200 W and 40 Hz for 300 s to produce small unilamellar liposomes.

Preparation of LPSF/AC04-CyDs-Loaded Liposomes

LPSF/AC04-CyDs-loaded liposomes were prepared as described above, but the aqueous phase consisted of a solution of pH 7.4 containing LPSF/AC04-HP-β-CyD or LPSF/AC04-HP-γ-CyD inclusion complexes, corresponding to 6 mg of LPSF/AC04.

Characterization of LPSF/AC04-CyDs-Loaded Liposomes

Stability of Liposomes

The stability of the liposomes was evaluated using a standard accelerated test. After preparation, samples of liposomal suspensions were submitted to centrifugation (3,165×*g* for 1 h at 4°C) and horizontal mechanical stirring (180 strokes/min for 48 h at 37°C). The pH of liposome dispersions was measured with a glass electrode and a digital pH meter (Bioblock Scientific 99622, Prolabo, Paris, France) at room temperature. Liposome dispersions were sized by photon correlation spectroscopy (Beckman Coulter Delsa™ Nano S Particle analyzer). Measurements were made at 25°C with a fixed angle of 90°, and sizes quoted are the mean of the liposomal hydrodynamic diameter. The polydispersity index was also measured using the same method and equipment.

Determination of Drug Content

An aliquot of liposomal sample (250 μl) was diluted to 10 ml with methanol, sonicated for 10 min, and an aliquot of 50 μl was diluted again with methanol to 5 ml. Samples were analyzed for determining the LPSF/AC04 content at 250 nm using a LPSF/AC04 standard curve with concentrations ranging from 0.5 to 3 μg/ml.

Entrapment Drug Efficiency

Drug entrapment efficiency (%EE) was determined by the ultrafiltration/ultracentrifugation technique, using Ultrafree® units (Millipore, USA). Samples of liposomes (400 μl) were inserted in the filtration unit and submitted to ultracentrifugation at 8,792×*g* for 1 h. The drug content was quantified in the supernatant, and the %EE was calculated according to Eq. 5. Data are presented as the percentage of the initial drug entrapped in liposomes.

$$\%EE = \frac{[LPSF/AC04\ content - unloaded\ LPSF/AC04]}{LPSF/AC04\ content} \times 100 \quad (5)$$

Antiproliferative Activity of LPSF/AC04 in Liposomal Formulations

The T47D (breast cancer) cell line obtained from ATCC was used in this study. The cells were maintained in RPMI-

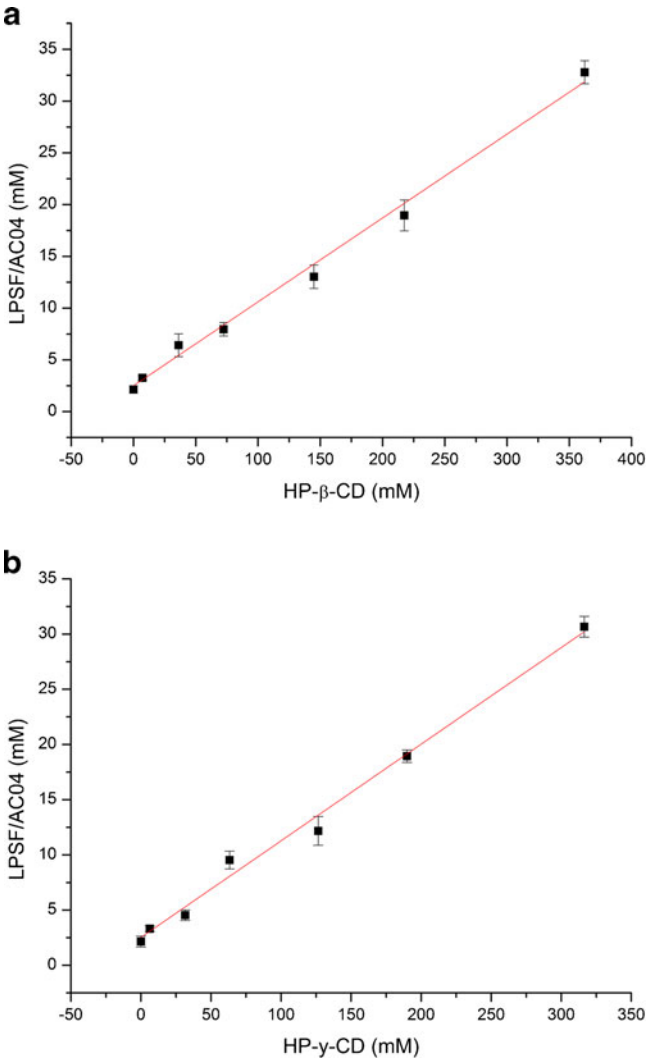

Fig. 2. Phase solubility diagram of LPSF/AC04 as a function of HP-β-CyD and HP-γ-CyD concentrations in water at 25°C. The linear fitting with regression analysis yielded: **a** $[LPSF/AC04]_{water}=0.1188\times[HP\text{-}\beta\text{-}CyD]+2.2701$ ($r^2=0.9923$) and **b** $[LPSF/AC04]_{water}=0.1295\times[HP\text{-}\gamma\text{-}CyD]+3.2416$ ($r^2=0.9961$)

1640 cell culture medium supplemented with 10% (FBS), streptomycin, and penicillin (all from Gibco Life Technologies, Paisley, UK). Culture was maintained at 37°C in an atmosphere of 5% CO_2. The antiproliferative activity of LPSF/AC04, LPSF/AC04–HP-β-CyD, and LPSF/AC04:HP-γ-CyD-loaded liposomes was evaluated on T47D cells using the MTT method (27). Cells were plated at (1×10^4 per well) on 96-well plates. After 24 h of incubation, cells were treated with serial concentrations of free LPSF/AC04 dissolved in DMSO, and samples of liposomes. Control cells were included and grown on each plate in the same conditions as treated cells. After incubation (72 h), 20 µl of MTT solution (5 mg/ml) was added to each well and incubated for 2 h. After this period, 100 µl of the medium was replaced by 130 µl of a sodium dodecylsulfate solution in HCl 0.01 M to dissolve the formazan crystals. The absorbance was read at 570 nm. The cytotoxicity was expressed as the concentration inhibiting 50% of cell proliferation (IC_{50}), which is the percentage reduction in cell viability calculated from the ratio between the number of cells treated with different LPSF/AC04 liposomal formulations and that of untreated cells (control).

Statistical Analysis

Statistical analyses of the data were performed using one-way ANOVA, followed by Tukey's multiple comparison test. A p value <0.05 was considered significant.

RESULTS

Phase Solubility Study of LPSF/AC04-Cyclodextrin Solutions

The phase solubility diagram of LPSF/AC04 in HP-β-CyD and HP-γ-CyD aqueous solutions showed A_L-curve types (Fig. 2a, b). Data were fitted by linear regression leading to the following equations: $[LPSF/AC04]_{water}=0.1188\times[HP-\beta-CyD]+2.2701\left(r^2=0.9923\right)$and $[LPSF/AC04]_{water}=0.1295\times[HP-\gamma-CyD]+3.2416\left(r^2=0.9961\right)$.

The solubility constants of LPSF/AC04 in HP-β-CyD and HP-γ-CyD solutions at 25°C were $K_{1:1}$=112.39 and 123.97, respectively, where the S_0=1.2 mM. The maximum enhancement of LPSF/AC04 solubility was achieved at 19 mM in HP-β-CyD and 17 mM in HP-γ-CyD, more than a tenfold increase over LPSF/AC04 solubility in water (1.2 mM). The CE of LPSF/AC04 in HP-β-CyD and HP-γ-CyD solutions, calculated according to Eq. 2, were 0.135 and 0.148, respectively (Table I).

Characterization of LPSF/AC04-CyD Inclusion Complexes

Vibrational and Raman Spectroscopic Analyses

The FTIR spectroscopy was used to verify the formation of LPSF/AC04 inclusion complexes with HP-γ-CyD and HP-β-CyD (Fig. 3). The FTIR results demonstrated the formation of LPSF/AC04–HP-β-CyD inclusion complexes, considering the decrease in the intensity of absorption bands of LPSF/AC04 functional groups (Fig. 3a). The FTIR spectrum of LPSF/AC04 shows the presence of bands at ~3,016 (C–H stretching vibration), 1,745 and 1,695 (C=O stretching), and 1,631 cm^{-1} (C=C stretching). The bands in the 1,425–1,300 cm^{-1} region are associated with the phenyl stretching vibration, and bands of the complexes in the 1,150–500 cm^{-1} region are due to C–H rocking vibrations of the rings and the

Table I. The Stability Constant ($K_{1:1}$) of the LPFS/AC04–HP-CyDs Inclusion Complexes, the Complexation Efficiency (CE), and Solubility Enhancement

Inclusion complexes	CE	$K_{1:1}$ (M^{-1}) using S_{int}	$K_{1:1}$ (M^{-1}) using S_0	LPSF/AC04 solubility enhancement (%)
LPSF/AC04–HP-β-CyD	0.135	59.45	112.39	19.07
LPSF/AC04–HP-γ-CyD	0.148	45.88	123.97	17.78

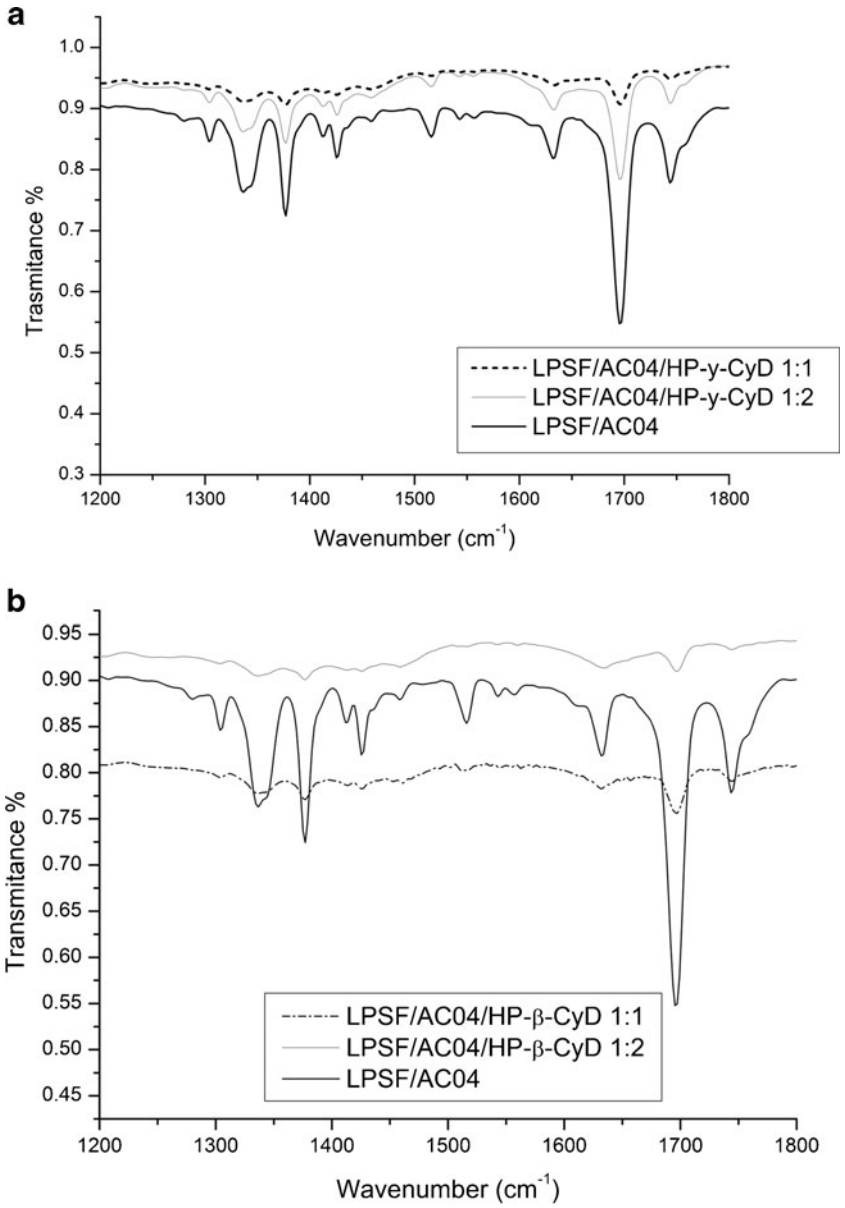

Fig. 3. FTIR spectra of LPSF/AC04 and LPSF/AC04–HP-γ-CyD (**a**), and LPSF/AC04 and LPSF/AC04–HP-β-CyD (**b**) inclusion complexes at 1:1 and 1:2 molar ratios

out-of-plane bending of aromatic C−H bonds. The FTIR spectra of HP-γ-CyD (Fig. 3a) and HP-β-CyD (Fig. 3b) are similar and show prominent absorption bands at ~3,411 (O−H stretching vibration), ~2,931 (C−H stretching vibration), ~1,157, ~1,089, and ~1,029 cm^{-1} (C−H and C−O stretching vibration). They present a large overlap of signals, with small changes in the intensity, broadenings, and shapes of the absorption bands, indicating the formation of complexes as new compounds, with typical fingerprint bands.

Similar results were found in Raman spectra of LPSF/AC04–HP-β-CyD (Fig. 4a, b) and of LPSF/AC04–HP-γ-CyD (Fig. 4c, d), demonstrating a change in the molecular environment of LPSF/AC04 in the inclusion complexes. The spectral regions found to be free of interfering CyD bands are particularly useful for highlighting the changes promoted by the inclusion process. These spectral regions are found above ca. 1,550 and ca. 3,000 cm^{-1} , which include some ring CC and the CH stretching modes ($\nu C\text{-}C_{ring}$ and $\nu C\text{-}H_{ring}$), respectively.

^{1}H-NMR Analysis

^{1}H-NMR experiments were performed to confirm the formation of LPSF/AC04–HP-CyDs inclusion complexes, evaluating the changes in the chemical shifts ($\Delta\delta$) of pure compounds (LPSF/AC04 and HP-β-CyD) and the LPSF/AC04:HP-CyDs inclusion complexes at the 1:1 and 1:2 molar ratios (Tables II, III, IV, and V). Chemical shift changes of H_3 and H_5 protons of HP-β-CyD were verified at both 1:1 ($\Delta\delta_{H3}$=0.015 and $\Delta\delta_{H5}$=0.012 ppm) and 1:2 ($\Delta\delta_{H3}$=0.012 and $\Delta\delta_{H5}$=0.011 ppm) molar ratios. These results indicated the potential of both 1:1 and 1:2 stoichiometry for the drug interactions with the inner cavity of cyclodextrins. However, other conformations

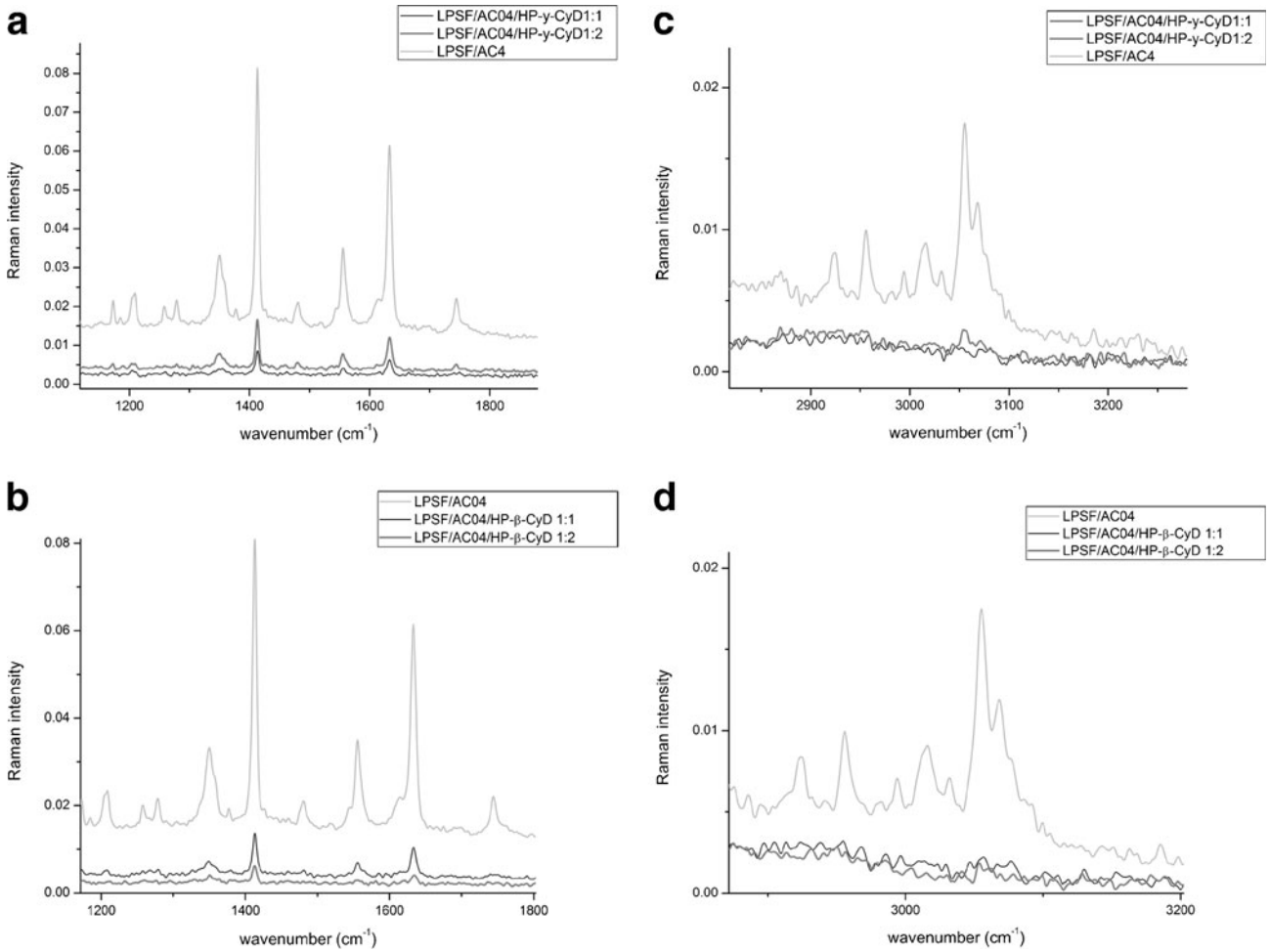

Fig. 4. Raman spectra of LPSF/AC04 and LPSF/AC04–HP-β-CyD inclusion complexes at 1:1 and 1:2 molar ratios and LPSF/AC04 and LPSF/AC04–HP-γ-CyD inclusion complexes at 1:1 and 1:2 molar ratios **a** and **b** 1,500–1,700 cm^{-1} region, **b** and **c** 2,800–3,200 cm^{-1} region

are not excluded, given that a higher chemical shift change in the H_4 proton was also observed ($\Delta\delta_{H4}$=0.018).

Thermal Analysis

The formation of LPSF/AC04–HP-β-CyD inclusion complexes was investigated by comparing the thermal behavior of 1:1 and 1:2 molar ratios. The DSC curve of LPSF/AC04 exhibited an endothermic peak corresponding to its melting temperature at 231.88°C with heat of reaction of −66.04 J/g (Fig. 5a). For the 1:1 and 1:2 LPSF/AC04–HP-β-CyD inclusion complexes, endothermic peaks at 231.40 and 231.17°C with heat of reaction of −15.62 and −8.45 J/g, respectively, were observed. The decrease in the heat of reaction is evidence of inclusion complex formation. The DT–TGA curves (Fig. 5b) showed an endothermic peak corresponding to the melting point of LPSF/AC04.On the other hand, in the case of the LPSF/AC04–HP-β-CyD inclusion complexes at molar ratios of 1:1 and 1:2, prominent peaks belonging to LPSF/AC04 completely disappeared. Furthermore, this behavior is an indication of interactions between LPSF/AC04 and CyDs in solid state. In addition, the thermogravimetric curves of the HP-β-CyD, LPSF/AC04, and LPSF/AC04–HP-β-CyD inclusion complexes at the 1:1 and 1:2 molar ratios (Fig. 5c) demonstrated the formation of the LPSF/AC04–HP-β-CyD inclusion complexes.

Scanning Electron Microscopy

The morphology of LPSF/AC04, HP-β-CyD, and LPSF/AC04–HP-β-CyD inclusion complexes was analyzed by SEM (Fig. 6). The LPSF/AC04 clearly presented an acicular crystalline form (Fig. 6a, a1), while HP-β-CyD (Fig. 6b, b1) is observed as cylindrical spheres. Both structures were in

Table II. ^{1}H-NMR Signals of HP-β-CyD and LPSF/AC04:HP-β-CyD at 1:2 Molar Ratio (Shifts Observed in Signals of HP-β-CyD)

HP-β-CyD	$\delta_{HP\text{-}\beta\text{-}CyD}$ (ppm)	$\delta_{LPSF/AC04\text{–}HP\text{-}\beta\text{-}CyD}$ (ppm)	$\Delta\delta$ (ppm)
H_1	5.093	5.084	0.011
H_2	3.696	3.696	0.000
H_3	3.935	3.923	0.012
H_4	3.395	3.386	0.018
H_5	3.491	3.502	0.011
H_6	3.804	3.802	0.002

HP-β-CyD and LPSF/AC04–HP-β-CyD in D_2O

Table III. ^{1}H-NMR Signals of HP-β-CyD and LPSF/AC04–HP-β-CyD at 1:1 Molar Ratio (Shifts Observed in Signals of HP-β-CyD)

HP-β-CyD	δ HP-β-CyD (ppm)	δ LPSF/AC04–HP-β-CyD (ppm)	Δδ (ppm)
H_1	5.093	5.083	0.010
H_2	3.696	3.693	0.003
H_3	3.935	3.920	0.015
H_4	3.395	3.384	0.011
H_5	3.491	3.479	0.012
H_6	3.804	3.799	0.005

HP-β-CyD and LPSF/AC04–HP-β-CyD in D_2O

accordance with previous data (28,29). On the other hand, images related to inclusion complex (Fig. 6c, c1) revealed a significant change in the morphology and shape of LPSF/AC04 and HP-β-CyD, presenting an amorphous form. Photomicrographs, in addition with the other results described above, demonstrate that interaction between the drug and cyclodextrin in inclusion complex.

Molecular Modeling Calculations

The inclusion complex between one LPSF/AC04 guest molecule and one HP-β-CyD host (1:1 LPSF/AC04–HP-β-CyD) was calculated in two ways: (1) the inclusion in HP-β-CyD was oriented by the toluene moiety and (2) the inclusion in HP-β-CyD was oriented by the acridine moiety. The most stable geometries found for the 1:1 LPSF/AC04–HP-β-CyD (toluene and acridine moieties) and 1:2 LPSF/AC04–HP-β-CyD inclusion complex can be observed in Fig. 7. The interaction energy ($\Delta E_{\text{bimolecular}}$) of the 1:1 LPSF/AC04–HP-β-CyD, determined by Eq. 3, is $-13.49\ \text{kJ mol}^{-1}$ for the inclusion complex oriented by the toluene moiety (Fig. 7a), and is $-27.74\ \text{kJ mol}^{-1}$ for the inclusion oriented by the acridine moiety (Fig. 7b). On the other hand, the interaction energy ($\Delta E_{\text{trimolecular}}$) of the 1:2 LPSF/AC04–HP-β-CyD determined by Eq. 4 is $-42.53\ \text{kJ mol}^{-1}$ (Fig. 7c).

Table IV. ^{1}H-NMR Signals of LPSF/AC04 and LPSF/AC04–HP-β-CyD at 1:2 Molar Ratio (Shifts Observed in Signals of LPSF/AC04)

LPSF/AC04	$\delta_{\text{LPSF/AC04}}$ (ppm)	$\delta_{\text{LPSF/AC04–HP-β-CyD}}$ (ppm)	Δδ (ppm)
H_e	8.767	8.775	0.008
H_a	8.242	8.249	0.007
	8.221	8.228	0.007
H_d	8.113	8.123	0.010
	8.092	8.100	0.008
H_b	7.924	7.929	0.006
	7.907	7.914	0.007
H_c	7.696	7.703	0.007
	7.676	7.685	0.009
H_g	7.347	7.356	0.009
	7.329	7.337	0.008
H_h	7.201	7.212	0.011
	7.185	7.193	0.008

HP-β-CyD and LPSF/AC04–HP-β-CyD in D_2O

Table V. ^{1}H-NMR Signals of LPSF/AC04 and LPSF/AC04–HP-β-CyD (Shifts Observed in Signals of LPSF/AC04) at Molar Ratio of 1:1

LPSF/AC04	$\delta_{\text{LPSF/AC04}}$ (ppm)	$\delta_{\text{LPSF/AC04–HP-β-CyD}}$ (ppm)	Δδ (ppm)
H_e	8.767	8,769	0.002
H_a	8.242	8.243	0.001
	8.221	8.221	0.000
H_d	8.113	8.115	0.002
	8.092	8.095	0.003
H_b	7.887	7.886	0.001
	7.907	7.907	0.000
H_c	7.696	7.696	0.000
	7.676	7.677	0.001
H_g	7.347	7.348	0.001
	7.329	7.331	0.002
H_h	7.201	7.201	0.000
	7.185	7.184	0.001

HP-β-CyD and LPSF/AC04–HP-β-CyD in D_2O

Characterization of LPSF/AC04 and LPSF/AC04–HP-CyDs-Loaded Liposomes

In the preformulation study of the encapsulation of LPSF/AC04 or its HP-CyDs inclusion complexes in liposomes, different batches were prepared by varying the drug/lipid molar ratio (1:21–1:48) and drug concentration (0.4–0.8 mg/ml). The most stable formulation of LPSF/AC04-loaded liposomes was obtained with a drug/lipid molar ratio of 1:28.76 corresponding to 0.6 mg/ml of LPSF/AC4 for 42 mM of lipids (PC/CHOL/SA, 7:2:1; Table VI). Based on these results, this formulation was chosen for further characterization (Table VII). The entrapment of LPSF/AC4 in the bilayer of liposomes (LP-LPSF/AC04) or the encapsulation of LPSF/AC04–HP-CyDs inclusion complexes in the aqueous cavity of liposomes (LP-LPSF/AC04–HP-β-CyD and LP-LPSF/AC04–HP-γ-CyD) has no influence on the size of liposomes (170 nm) or drug encapsulation efficiency (93%).

Antiproliferative Activity of LPSF/AC04 in Liposomal Formulations

The antiproliferative activity of LPSF/AC04 and LPSF/AC04–HP-CyDs inclusion complexes encapsulated in liposomes in T47D cell, expressed as cell viability (percentage), is shown in Fig. 8. The 50% growth inhibitory concentration (IC_{50}) was estimated from the available cytotoxicity data, and results are given in Table VIII. IC_{50} values of 82.57 ± 9.26 and $65.06 \pm 5.95\ \mu M$ were found for free LPSF/AC04 and encapsulated LP-LPSF/AC04, respectively. On the other hand, IC_{50} values of 35.00 ± 13.6 and $32.00 \pm 14.8\ \mu M$ were found for the liposomal formulations containing inclusion complexes (LP-LPSF/AC04–HP-β-CyD and LP-LPSF/AC04–HP-γ-CyD), respectively. Statistically significant differences ($p < 0.05$) between LPSF/AC04, LPSF/AC04-loaded liposomes, and LPSF/AC04–HP-CyD-loaded liposomes were confirmed by ANOVA.

Taken together, the results demonstrated that when LPSF/AC04 was incorporated into liposomes, an increase in drug penetration into the cells occurred, and the cytotoxicity

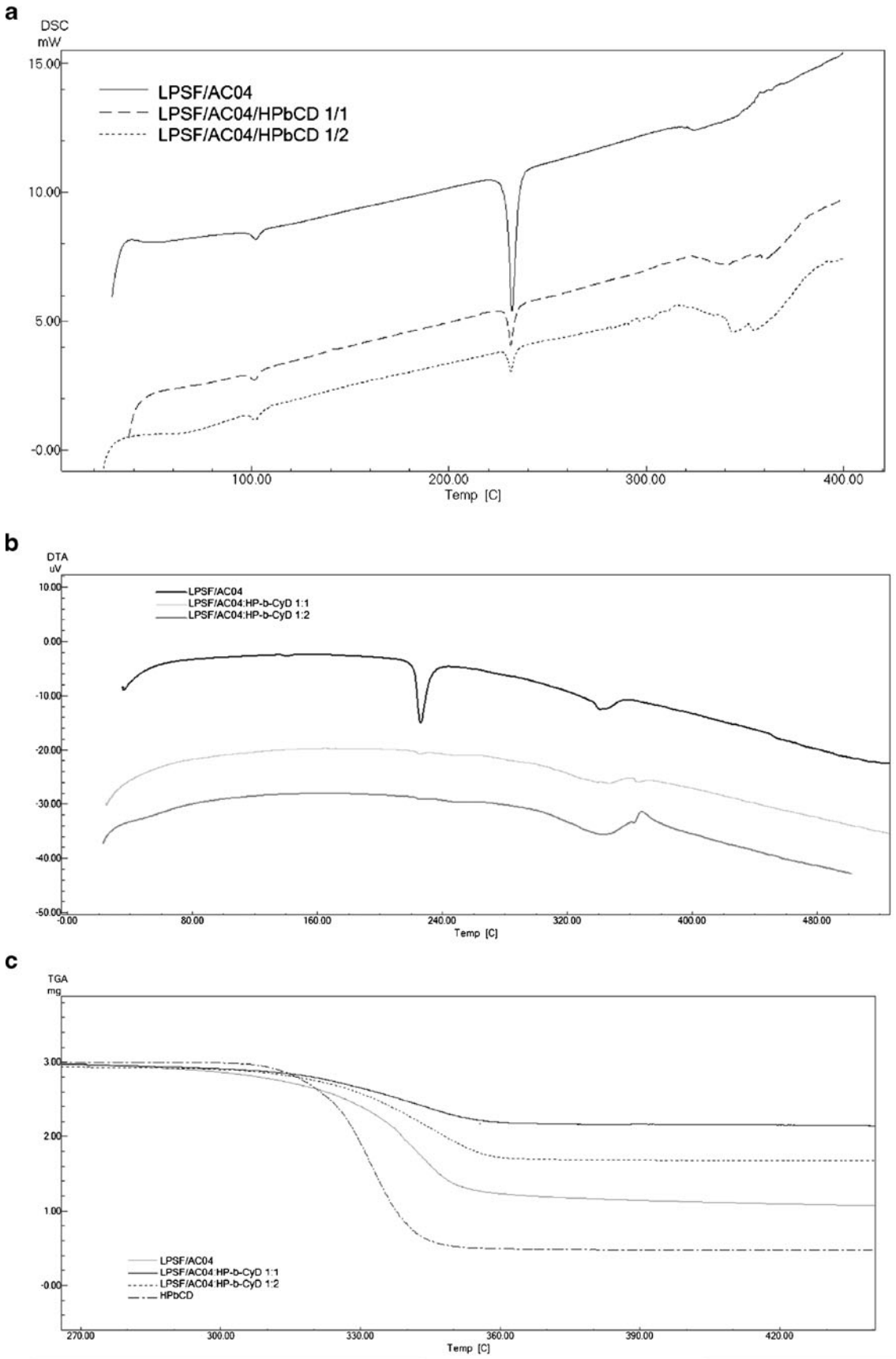

Fig. 5. Simultaneous (DSC) (**a**), (DTA) (**b**), and TG (**c**) curves of LPSF/AC04 and LPSF/AC04–HP-β-CyD inclusion complexes at 1:1 and 1:2 molar ratios

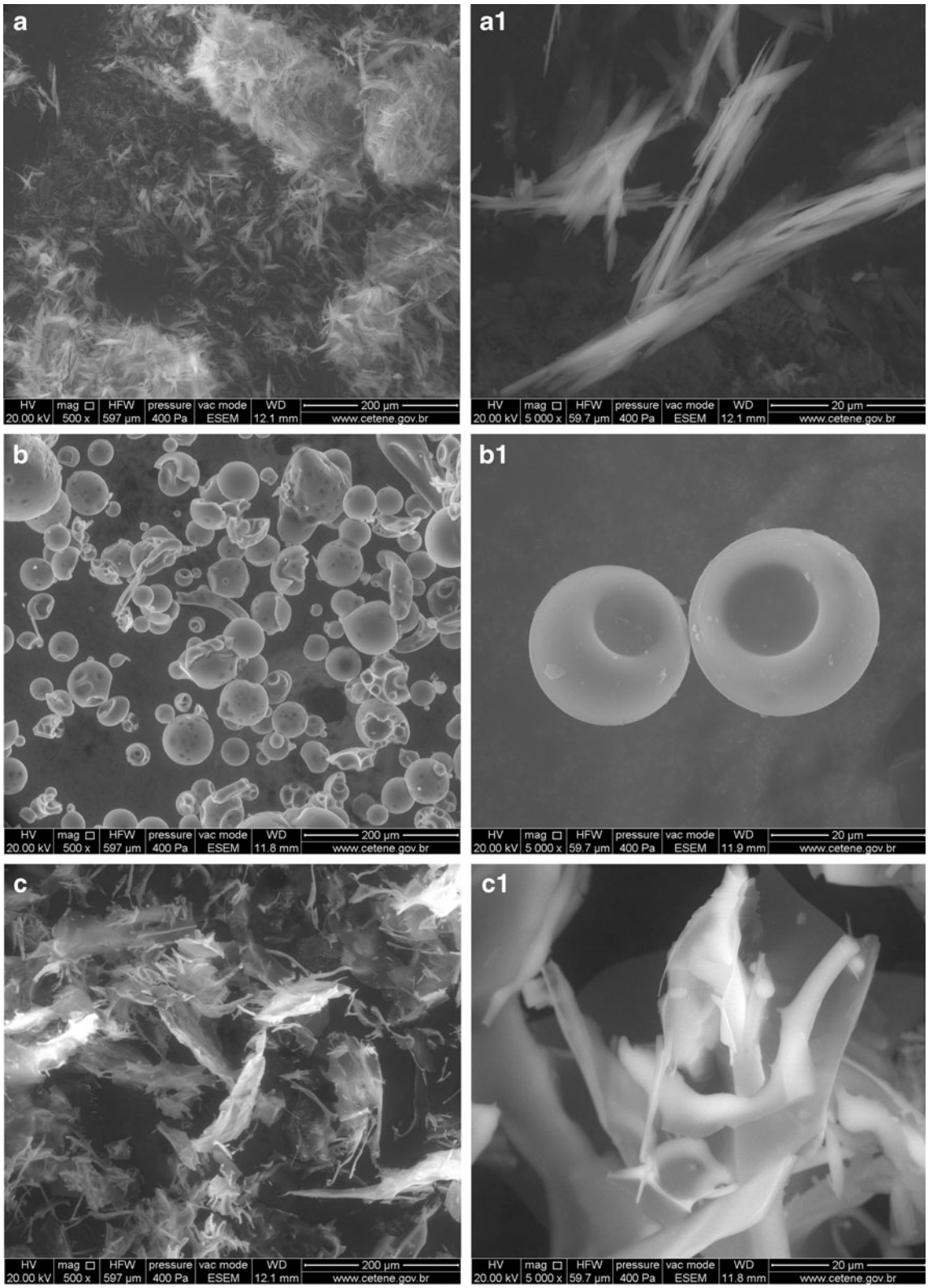

Fig. 6. SEM photographs of LPSF/AC04 (**a**, **a1**), HP-β-CyD (**b**, **b1**), and LPSF/AC04–HP-β-CyD (**c**, **c1**)

activity increased. Moreover, these results clearly demonstrated that the incorporation of LPSF/AC04–HP-β-CyD inclusion complexes into liposomes increased twofold the cytotoxicity activity over LPSF/AC04-loaded liposomes.

DISCUSSION

The main focus of the present study was to improve the solubility of LPSF/AC04 in cyclodextrins through the

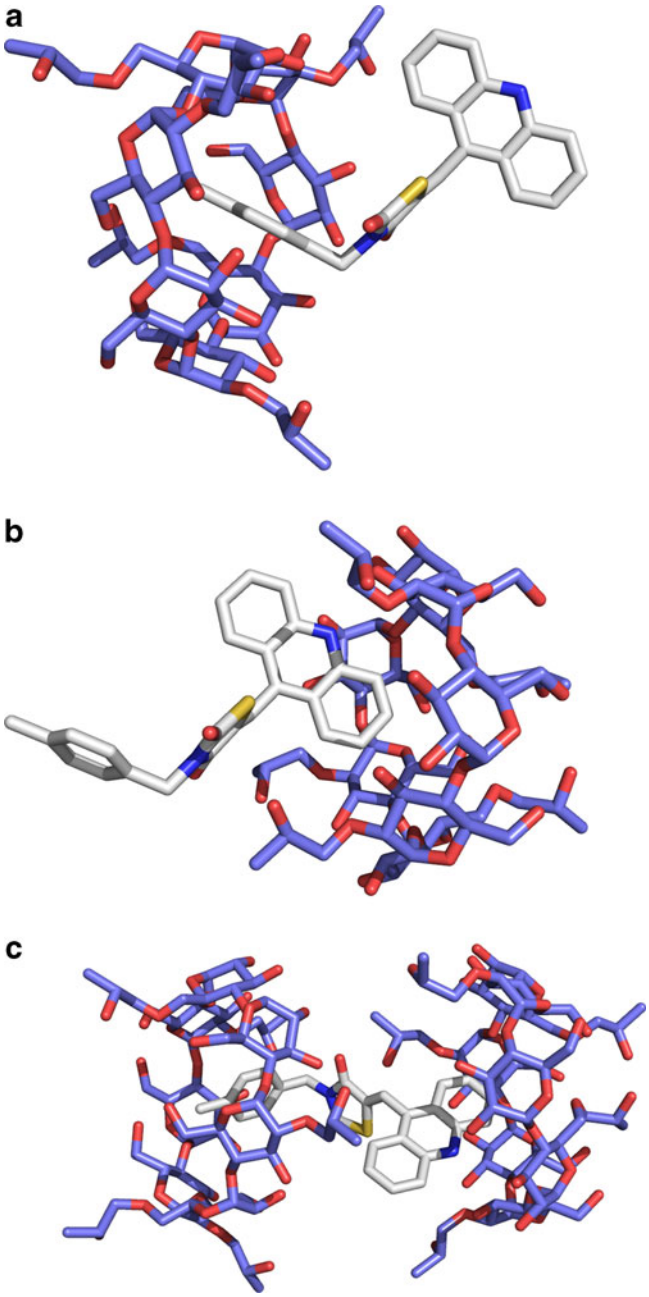

Fig. 7. Optimized geometries found for 1:1 LPSF/AC04–HP-β-CyD inclusion complex formed by **a** toluene and **b** acridine moieties, and **c** LPSF/AC04–HP-β-CyD 1:2 inclusion complex

formation of inclusion complexes and their encapsulation into liposomes for evaluating the antiproliferative activity. A physicochemical characterization and molecular modeling calculations of LPSF/AC04–CyDS inclusion complexes were also performed. According to the literature, phase solubility analysis is one of the preliminary requirements for developing a drug/cyclodextrin inclusion complex as it permits an evaluation of the affinity between the drug molecule and cyclodextrin (21). Many researchers have used this approach to determine the molar ratio in which a drug can form a complex with cyclodextrins (11–14). However, the phase solubility profiles do not demonstrate the formation of inclusion complexes; they only describe how the increasing cyclodextrin concentration influences drug solubility. Loftsson and co-workers (9)

Table VI. Pre-formulation Study of Liposomes Containing LPSF/AC04 in a Suspension Dosage Form

Drug/lipid molar ratio (PC/CHOL/SA, 42 mM)	[LPSF/AC04] (mg/mL)	Micro and macroscopic appearance	Time (days)
1:43.29	0.4	Stable	60
1:28.76	0.6	Stable	90
1:21.53	0.8	Unstable[a]	11

[a] Unstable = precipitation of LPSF/AC04 with the presence of LPSF/AC04 crystals

have reported that a more accurate method for determining the solubilizing efficiency of cyclodextrins is to calculate the CE. CE is calculated from the slope of the phase solubility diagrams, which is independent of both S_0 and S_{int}. If CE is 0.1, then 1 out of every 11 cyclodextrin molecules forms a complex with the drug, and if CE is 0.01, then only 1 out of every 100 cyclodextrin molecules forms a complex. The results of the solubility constant and CE of the LPSF/AC04–HP-β-CyD and LPSF/AC04:HP-γ-CyD inclusion complexes (Table I) suggest that only a small amount of LPSF/AC04 is in a noncomplexed form in the LPSF/AC04–HP-β-CyD and LPSF/AC04–HP-γ-CyD inclusion complexes.

From the analysis of the FTIR and Raman spectra, we have been able to suggest the formation, in solid phase, of the LPSF/AC04–HP-γ-CyD and LPSF/AC04–HP-β-CyD inclusion complexes, based on the observations of decreases in the intensity of absorption bands of functional LPSF/AC04 groups that were affected by interactions with the cyclodextrins. They present a large overlap of signals, with small changes in the intensity, broadenings, and shapes of the absorption bands that indicate the formation of complexes as new compounds, with typical fingerprint bands (30). In addition, of the four inclusion complexes examined, the 1:2 LPSF/AC04–HP-β-CyD was considered the most stable, due to its greater ability to mitigate the signals of the functional AC04 groups. The 1:1 LPSF/AC04–HP-β-CyD inclusion complex was the second most stable, followed by 1:1 and 1:2 LPSF/AC04–HP-γ-CyD. This order of attenuation can be best observed in the region between 1,200 and 1,800 cm^{-1} that corresponds to the C=O and C=C stretching, and to the phenyl stretching vibration of the LPSF/AC04 molecule.

Raman spectroscopy has provided evidence of the success of inclusion complex formation by means of a comparison between the spectra of LPSF/AC04 molecule and the spectra of the inclusion complex. The first indication of a change in the molecular environment of LPSF/AC04 in the inclusion complex is the broadening of the Raman bands, specially by the analysis of the 1,500–1,700 cm^{-1} region (Fig. 4a, b) and 2,800–3,200 cm^{-1} region (Fig. 4c, d) (31). The combined results of Raman and FTIR confirm the inclusion compound and also that LPSF/AC04:HP-β-CyD is relatively more stable than the LPSF/AC04:HP-γ-CyD inclusion complex, hence the choice of the LPSF/AC04:HP-β-CyD complex for further investigation.

The ^{1}HNMR studies confirmed that, in the presence of LPSF/AC04, the H3 and H5 protons of the HP-β-CyD cavity are up-field shifted, suggesting that the LPSF/AC04 molecule is included inside the HP-β-CyD cavity, with a potential 1:1 and 1:2 stoichiometry ratio. In fact, drug inclusion complexes

Table VII. Liposomes Containing LPSF/AC04 in a Suspension Dosage Form

Formulations	Size (nm)	Polydispersity index (PI)	Entrapment efficiency (EE) (%)
LPSF/AC04-LP	189.05±7.9	0.39±0.02	91.89±1.2
LPSF/AC04–HP-β-CyD-LP	153.50±3.2	0.28±0.05	93.57±0.37
LPSF/AC04–HP-γ-CyD-LP	179.63±2.1	0.45±0.03	94.02±0.27

of the both 1:1 and 1:2 molar ratios would be expect to be formed. In addition, 1:1 or 1:2 cyclodextrin inclusion complexes form water-soluble aggregates in aqueous solutions, and these aggregates are able to solubilize lipophilic water-insoluble drugs through non-inclusion complexation or micelle-like structures (32).

The TGA and DTG results of LPSF/AC04–HP-β-CyD inclusion complexes compared to the pure compounds LPSF/AC04 and HP-β-CyD could be considered as evidence of a successful complexation because the melting point is determined by the intermolecular interactions stabilizing the crystalline structure of the compound. Additionally thermal stability is probably due to the formation of the LPSF/AC04–HP-β-CyD inclusion complex.

The SEM analysis shows a change from the crystalline to amorphous form of LPSF/AC04 and HP-β-CyD, in complexed form (Fig. 6), revealing an apparent interaction between the drug and the cyclodextrin. This phenomenon was then corroborated by molecular modeling, which demonstrated that the main intermolecular interactions occur between the N and C=O acceptor groups of the guest molecule (LPSF/AC04) and the OH donor groups of the host molecule (HP-β-CyD). These important polar interactions constitute the main intermolecular reasons for the stability of the 1:1 and 1:2 LPSF/AC04–HP-β-CyD inclusion complexes.

Based on the results of the preformulation studies, the liposome formulation with the highest stability as well as the largest amount of drug loading was prepared with a 1:29 drug/lipid molar ratio. In this way, liposomes containing LPSF/AC04 or LPSF/AC04–HP-CyD inclusion complexes were obtained with a lipid concentration of 42 mM and LPSF/AC04 at 0.6 mg/ml. LP-LPSF/AC04 and LP-LPSF/AC04–HP-CyD in suspension form presented homogeneous particle size distributions on the nanometer scale, as well as stability for over 90 days. Moreover, both formulations presented a particle size of 170 nm, which is suitable for tumor targeting.

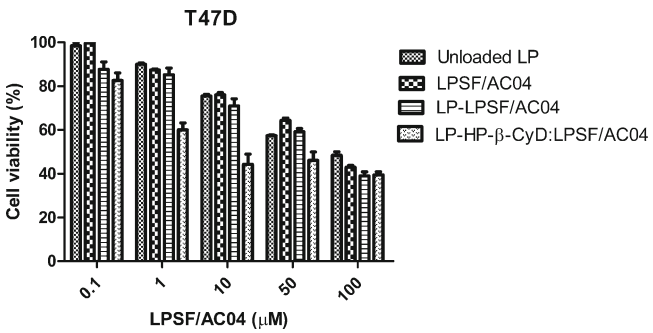

Fig. 8. Antiproliferative activity of liposomal formulations of LPSF/AC04, LPSF/AC04–HP-β-CyD, and LPSF/AC4–HP-γ-CyD on T47D cell line. Data represent the mean of three separate experiments±SD (n=9)

The antiproliferative activity of LP-LPSF/AC04 and LP-LPSF/AC04–HP-CyD was evaluated in T47D. The results showed that both liposomal formulations induced a dose-dependent cytotoxicity. LPSF/AC04–HP-CyD-LP inhibits T47D cell proliferation stronger than free LPSF/AC04, and twofold that of LPSF/AC04-loaded liposomes. Several studies have also shown that either free or encapsulated drug inclusion complexes into liposomes enhanced the cytotoxicity compared to the pure molecule. In addition, the difference observed in the cell proliferation may be explained on the basis of the CyD properties (33–35).

This is the first report that demonstrated the both dosage form strategies for the anticancer candidate LPSF/AC04, entrapment of into the phospholipid bilayer of liposomes, or the incorporation of LPSF/AC04–HP-CyD inclusion complexes in the aqueous cavity of liposomes leading to an increase in its cytotoxicity probably due to cell penetration. Data evaluation revealed that liposomal LPSF/AC04 maintains and liposomal LPSF/AC04–HP-CyD enhances the LPSF/AC04 property as an antiproliferative agent. This is in agreement with the results of Dhule and co-workers (35), which describe that CyD complexation enhances curcumin solubilization and increases its encapsulation into the aqueous liposomal cavity. In addition, the antiproliferative activity of curcumin was increased by cyclodextrin complexation and encapsulation into liposomes. Moreover, our recent researches have reported that the solubilization of the anticancer agents usnic acid and β-lapachone with cyclodextrins and their encapsulation into liposomes offer a way to improve drug solubility (19,20).

The large number of reports in the literature demonstrating that anticancer molecules have enhanced their effect, as a result of complexation with cyclodextrins, encourages us to study the solubility of LPSF/AC04 in the presence of CyDs. Our results demonstrate that the nanoencapsulation of LPSF/AC04–HP-β-CyD inclusion complexes into liposomes leads to enhance the effects of antitumor activity.

Table VIII. IC_{50} of Free and Encapsulated LPSF/AC04 Antiproliferative Activities

IC_{50} (μM)	
	Cell line
Samples	T47D
LPSF/AC04	82.57±9.26
LP_LPSF/AC04	65.06±5.95
LP_LPSF/AC04:HP-β-CyD	35.00±13.6
LP_LPSF/AC04:HP-γ-CyD	32.00±14.8

Mean of values of three separate experiments (n=9)±SD

CONCLUSIONS

The present study shows the intermolecular interactions in the LPSF/AC04–HP-β-CyD inclusion complexes studied by molecular modeling. Our results confirm the hypothesis that inclusion complexes of LPSF/AC04 with HP-β-CyD and HP-γ-CyD are formed and that the LPSF/AC04–HP-β-CyD complexes are more stable than LPSF/AC04–HP-γ-CyD. These findings showed that the nanoencapsulation of LPSF/AC04–HP-β-CyD into liposomes is an alternative means of overcoming drug poor solubility, as well as probably improving drug penetration into the cells and enhancing drug antiproliferative activity. Further *in vivo* studies comparing the LPSF/AC-04 and LPSF/AC04–HP-β-CyD inclusion complexes encapsulated in liposomes will be conducted to corroborate the results of this investigation.

ACKNOWLEDGMENTS

The thermal analyses were performed at the Pharmaceutical Technology Laboratory of the UFPE Department of Pharmacy, with the kind collaboration of Dr. Pedro Rolim and the much appreciated technical assistance of Mrs. Larissa Rolim.

REFERENCES

1. Denny WA. Acridine derivatives as chemotherapeutic agents. Curr Med Chem. 2002;9:1655–65.
2. Goodell JR, Ougolkov AV, Hiasa H, Kaur H, Remmel R, Billadeu DD, *et al*. Acridine-based agents with topoisomerase II activity inhibit pancreatic cancer cell proliferation and induce apoptosis. J Med Chem. 2008;51:179–82.
3. Vispe S, Vandenberghe I, Robin M, Annereau JP, Créancier L, Pique V, *et al*. Novel tetra-acridine derivatives as dual inhibitors of topoisomerase II and the human proteasome. Biochem Pharmacol. 2007;73:1863–72.
4. Loise AC, Issel BF. Amsacrine (AMSA)—a clinical review. J Clin Oncol. 1985;3:562–92.
5. Chilin A, Marzaro G, Marzano C, Via LD, Ferlin MG, Pastorin G, *et al*. Synthesis and antitumor activity of novel amsacrine analogs: the critical role of the acridine moiety in determining their biological activity. Bioorg Med Chem. 2009;17:523–9.
6. Mourão RH, Silva TG, Soares AL, Vieira ES, Santos JN, Lima MCA, *et al*. Synthesis and biological activity of novel acridinylidene and benzylidene thiazolidinediones. Eur J Med Chem. 2005;40:1129–33.
7. Pitta IR, Galdino SL, Lima MCA. Acridine derivatives with antitumoral activity. Patent number WO/2007/109871. PCT/BR2007/000074. 2007.04.10. Federal University of Pernambuco, Recife, Brazil.
8. Pigatto MC, Lima MCA, Galdino SL, Pitta IR, Vessecchi R, Assis MD, *et al*. Metabolism evaluation of the anticancer candidate AC04 by biomimetic oxidative model and rat liver microsomes. Eur J Med Chem. 2011;46:4245–51.
9. Loftsson T, Hreinsdóttir D, Másson M. Evaluation of cyclodextrin solubilization of drugs. Int J Pharm. 2005;302:18–28.
10. Loftsson T, Duchêne D. Cyclodextrins and their pharmaceutical applications. Int J Pharm. 2007;329:1–11.
11. Schuette JM, Dou TN, de la Peña AM, Greene KL, Williamson CK, Warner IM. Characterization of the β-cyclodextrin/acridine complex. J Phys Chem. 1991;95:4897–902.
12. Correia I, Bezzenine N, Ronzani N, Platzer N, Beloeil J-C, Doan B-T. Study of inclusion complexes of acridine with β-and (2,6-di-*o*-methyl)-β-cyclodextrin by use of solubility diagrams and NMR spectroscopy. J Phys Org Chem. 2002;15:647–59.
13. Mishur RJ, Griffin ME, Battle CH, Shan B, Jayawickramrajah J. Molecular recognition and enhancement of aqueous solubility and bioactivity of CD437 by β-cyclodextrin. Bioorg Med Chem Lett. 2011;21:857–60.
14. Al Omari AA, Al Omari MM, Badwan AA, Al-Sou'od KA. Effect of cyclodextrins on the solubility and stability of candesartan cilexetil in solution and solid state. J Pharm Biomed Anal. 2011;54:503–9.
15. Torchilin VP. Multifunctional nanocarriers. Adv Drug Deliv Rev. 2006;58:1532–55.
16. McCormack B, Gregoriadis G. Drugs-in-cyclodextrins-in-liposomes: an approach to controlling the fate of water insoluble drugs *in vivo*. Int J Pharm. 1998;162:59–69.
17. Loukas YL, Vraka V, Gregoriadis G. Drugs, in cyclodextrins, in liposomes: a novel approach to the chemical stability of drugs sensitive to hydrolysis. Int J Pharm. 1998;162:137–42.
18. Maestrelli F, Gonzalez-Rodriguez ML, Rabasco AM, Mura P. New "drug-in cyclodextrin-in deformable liposomes" formulations to improve the therapeutic efficacy of local anesthetics. Int J Pharm. 2010;395:222–31.
19. Lira MCB, Ferraz MS, da Silva DGVC, Cortes ME, Teixeira KI, Caetano NP, *et al*. Inclusion complex of usnic acid with β-cyclodextrin: characterization and nanoencapsulation into liposomes. J Incl Phenom Macrocycl Chem. 2009;64:215–24.
20. Cavalcanti IMF, Mendonça EAM, Lira MCB, Honrato SB, Amorim C, Amorim RVS, *et al*. The encapsulation of β-lapachone in 2-hydroxypropyl-β-cyclodextrin inclusion complex into liposomes: a physicochemical evaluation and molecular modeling approach. Eur J Pharm Sci. 2011;44:332–40.
21. Higuchi T, Connors KA. Phase-solubility techniques. Adv Anal Chem. 1965;4:117–212.
22. Mura P, Bettinetti G, Melani F, Manderioli A. Interaction between naproxen and chemically modified β-cyclodextrins in the liquid and solid state. Eur J Pharm Sci. 1995;3:347–55.
23. Aicart E, Junqueira E. Complex formation between purine derivatives and cyclodextrins: a fluorescence spectroscopy study. J Incl Phenom Macrocycl Chem. 2003;47:161–5.
24. Illapakurthy AC, Sabnis YA, Avery BA, Avery MA, Wyandt CM. Interaction of artemisinin and its related compounds with hydroxypropyl-β-cyclodextrin in solution state: experimental and molecular-modeling studies. J Pharm Sci. 2003;92:649–55.
25. Araújo MVG, Vieira EKB, Lázaro GS, Conegero LS, Almeida LE, Barreto LS, *et al*. Sulfadiazine/hydroxypropyl-β-cyclodextrin host–guest system: characterization, phase-solubility and molecular modeling. Bioorg Med Chem. 2008;16:5788–94.
26. Hao SY, Molnar LF, Jung Y, Kussmann J, Ochsenfeld C, Brown ST, *et al.* Advances in methods and algorithms in a modern quantum chemistry program package. Phys Chem Chem Phys. 2006;8:3172–91.
27. Mosmann T. Rapid colorimetric assay for cellular growth and survival: application of proliferation and cytotoxicity assay. J Immunol Methods. 1983;65:55–63.
28. Pralhad T, Rajendrakumar K. Study of freeze-dried quercetin–cyclodextrin binary systems by DSC, FT-IR, X-ray diffraction and SEM analysis. J Pharm Biomed Anal. 2004;34:333–9.
29. Ribeiro A, Figueiras A, Santos D, Veiga F. Preparation and solid-state characterization of inclusion complex formed between miconazole and methyl-β-cyclodextrin. AAPS PharmSciTech. 2008;9:1102–9.
30. Aigner Z, Berkesi O, Farkas G, Szabo-Revesz P. DSC, X-ray and FTIR studies of a gemfibrozil/dimethyl-β-cyclodextrin inclusion complex produced by co-grinding. J Pharm Biomed Anal. 2012;57:62–7.
31. Sardo M, Amado AM, Ribeiro-Claro PJA. Inclusion compounds of phenol derivatives with cyclodextrins: a combined spectroscopic and thermal analysis. J Raman Spectrosc. 2009;40:1624–33.
32. Loftsson T, Masson M, Brewster ME. Self-association of cyclodextrins and cyclodextrin complexes. J Pharm Sci. 2004;93:1091–9.
33. Upadhyay AK, Singh S, Chhipa RR, Vijayakumar MV, Ajay AK, Bhat MK. Methyl-β-cyclodextrin enhances the susceptibility of human breast cancer cells to carboplatin and 5-fluorouracil: involvement of Akt, NF-κB and Bcl-2. Toxicol Appl Pharmacol. 2006;2:177–85.
34. Pourgholami MH, Wangoo KT, Morris DL. Albendazole–cyclodextrin complex: enhanced cytotoxicity in ovarian cancer cells. Anticancer Res. 2008;28:2775–80.
35. Dhule SS, Penfornis P, Frazier T, Walker R, Feldman J, Tan G, *et al*. Curcumin-loaded γ-cyclodextrin liposomal nanoparticles as delivery vehicles for osteosarcoma. Nanomedicine. 2012;8:440–51. doi:10.1016/j.nano2011.07.011.